Conformal cubical 3D transformation-based metamaterial invisibility cloak

Slobodan V. Savić,[1] Branislav M. Notaroš,[2,*] and Milan M. Ilić[1,2]

[1]*School of Electrical Engineering, University of Belgrade, Belgrade 11120, Serbia*
[2]*Department of Electrical and Computer Engineering, Colorado State University, Fort Collins, Colorado 80523-1373, USA*
Corresponding author: notaros@colostate.edu

A conformal cubical transformation-based metamaterial invisibility cloak is presented and verified, in the near and the far field, by a rigorous full-wave numerical technique based on a higher-order, large-domain finite element method, employing large anisotropic, continuously inhomogeneous generalized hexahedral finite elements, with no need for discretization of the permittivity and permeability profiles of the cloak. The analysis requires about 30 times fewer unknowns than with commercial software. To our knowledge, this is the first conformal cubical cloak and the first full-wave computational characterization of such a structure with sharp edges. The presented methodology can also be used in development of conformal, transformation-based perfectly matched layers.   © 2012 Optical Society of America

OCIS codes: 000.4430, 230.3205, 260.2110, 290.5839.

1. INTRODUCTION

Transformation optics (or transformation electromagnetics) has recently become one of the mainstream areas of theoretical and applied optics (electromagnetics). Of particular and emerging interest, at both optical wavelengths and RF/microwave frequencies, are transformation-based metamaterials, which possess novel wave material interaction properties not possible with "standard" or natural media. Transformation-optics techniques use the invariance property of Maxwell's equations under coordinate transformations to control the electromagnetic fields, namely, to guide optical paths (or lines of the Poynting vector), in a desired fashion, and the application of such techniques that has received the greatest attention so far is the design of transformation-based metamaterial invisibility cloaks. Essentially, the transformations are employed to reshape the original coordinate system (and thus redirect the optical paths) in order to create a void region (spatial region that is not spanned by any curved coordinate lines) in the new coordinate system, which is going to be invisible for observation locations outside the cloak, with the newly formed spatial curvatures then being transformed into the corresponding scaling of medium parameters (permittivity and permeability tensors). The resulting materials for the cloaks turn out to be continuously inhomogeneous and anisotropic.

As far as the shape of transformation-based metamaterial invisibility cloaks is concerned, circular cylindrical two-dimensional (2D) cloaks are designed and evaluated (analytically and/or numerically) in [1], while the designs and evaluations of spherical three-dimensional (3D) cloaks appear in [2,3]. For these (regular) shapes, material parameters can easily be expressed in a closed form, and the resulting continuously inhomogeneous and anisotropic cloaks with radially varying permittivity and permeability tensors can be analyzed using analytical exact methods (e.g., Mie

scattering analytical model of spherical cloaks [4,5]). Approaches for construction and analysis of transformation-based cloaks with other (arbitrary) shapes have been investigated as well. Most theoretical considerations of such cloaks are based on a straight-line compression of space, where there exists at least one point inside the cloak's void region positioned so that all of the cloak's outer surface points could be reached from it along straight lines inside the cloak [6,7]. A more general approach is considered in [8], where the coordinate transformation is represented in the form of a homogeneous topological mapping where possible, while in the case of cloaks with arbitrary (potentially complex) shapes, for which homogeneous topological mapping functions cannot be (easily) obtained in a closed form, an approximation approach is proposed. Coordinate transformations for irregular particles in the form of ellipsoids, rounded cuboids, and rounded cylinders, respectively, are studied in [9], where the scattered field distribution is simulated using the discrete dipole approximation. As far as transformation-based metamaterial invisibility cloaks with sharp edges and corners are considered, on the other hand, [10] provides a design and demonstration of a square 2D (cylinder with a square-shaped cross section) cloak. To the best of our knowledge, a generalization of this approach to the corresponding 3D case, namely, to a construction, analysis, and evaluation of a cubical 3D cloak, is lacking in the rich and growing literature and body of knowledge on invisibility cloaks based on transformation optics (electromagnetics).

This paper presents a novel conformal cubical transformation-based metamaterial invisibility cloak and its rigorous full-wave numerical validation and evaluation using higher-order, large-domain anisotropic continuously inhomogeneous material modeling based on a hybridization of the finite element method (FEM) for the cloaking region and the method of moments (MoM) for the termination of the

computational domain. The cloak is constructed invoking a classical coordinate transformation, similar to that in [10]. The numerical characterization is carried out employing the FEM–MoM modeling approach and tool proposed for the analysis of cloaking structures in [3], which implements large anisotropic continuously inhomogeneous generalized hexahedral finite elements, so there is no need for a discretization of the permittivity and permeability profiles of the cloak (subdivision into very small finite elements), typical for all other approaches to FEM analysis of transformation-based metamaterial cloaks. This appears to be the first cubical cloak and the first full-wave computational electromagnetic characterization of such a structure with sharp edges and corners. Given that some possible future applications of cloaking devices would likely include thin (for practical reasons) conformal cloaking layers on complex 3D geometries, we focus in the paper mainly on thin cloaks. The cloaking performance is analyzed in both the near field and the far field, and for both lossless and lossy (for different loss tangents) cloaks, over a broad range of wavelengths. We show that both lossless and lossy cloaks introduce significant reductions (five to ten orders of magnitude) in the backscattering cross section of the cloaked cube in the entire analyzed range of wavelengths, and that a simple 24-element large-domain FEM model of the cubical cloak efficiently yields excellent results in comparison with alternative full-wave numerical solutions obtained by commercial software (the reduction in the required number of unknowns is by about 30 times).

Additionally, we emphasize that, for all situations where conformal cloaks for cloaking of objects with sharp edges and corners are employed, a full-wave numerical analysis is unavoidable, as these problems cannot be treated by the Mie scattering theory or any other analytical method. This is always the case with complex 3D real-world geometries. Therefore, as an additional goal, we investigate the capabilities of our continuously anisotropic higher-order FEM–MoM technique in this specific (numerically demanding) case, of a cubical cloak, noting that practically all of the works that include full-wave numerical characterizations of various metamaterial cloaks rely on COMSOL Multiphysics (e.g., [1,10]), which employs small-domain low-order discretizations and piecewise homogeneous approximations of continuously varying material parameters in finite elements that are deemed inefficient.

Finally, the presented novel cubical cloak and its rather unconventional validation and evaluation can be of significant interest to researchers seeking coordinate transformations needed for the conformal cloaking of cubical structures or for similar (more complex) structures with sharp edges and corners. Moreover, this study may be of great importance for the development of conformal transformation-based perfectly matched layers (PMLs), as mathematical concepts, used for local-type truncations of finite element meshes in FEM-based codes for numerical analysis of electromagnetics/optics phenomena. It may also serve as a starting point for development of the respective reduced-parameter invisibility cloaks, constructed from isotropic homogeneous material layers and thus potentially enabling a simpler experimental demonstration [11,12], which, in turn, may be treated (based on the effective medium approximation) as an effective anisotropic medium (e.g., [11]).

2. CONSTRUCTION AND NUMERICAL FEM–MoM MODELING OF A CUBICAL CLOAK

To construct a 3D cubical cloak, we start by introducing a simple coordinate transformation that maps the original Cartesian coordinate system (transformation domain), with x, y, z coordinates [Fig. 1(a)], into a transformed one (transformation range), with x', y', z' coordinates [Fig. 1(b)]:

$$x' = R_1 + \frac{R_2 - R_1}{R_2}x, \qquad y' = y\left(\frac{R_2 - R_1}{R_2} + \frac{R_1}{x}\right),$$

and $\quad z' = z\left(\frac{R_2 - R_1}{R_2} + \frac{R_1}{x}\right),$ (1)

where R_1 and R_2 represent half-side lengths of the inner and the outer cubical shells, respectively. Note that the transformation given in Eq. (1) can be considered as a generalization of the transformation for the square 2D cloak construction [10]. It maps one sixth of the original homogeneous isotropic (air filled in our case) cube ($0 < x \leq R_2$, $-R_2 \leq y \leq R_2$, $-R_2 \leq z \leq R_2$, and $|y|, |z| < |x|$) to one sixth of the transformed cubical shell ($R_1 < x' \leq R_2$, $-R_2 \leq y' \leq R_2$, $-R_2 \leq z' \leq R_2$, and $|y'|, |z'| < |x'|$), as shown by the shaded regions in Fig. 1, and similarly for the mappings of the remaining five parts of the cubical shell. This way, a hole [free of any exterior field and marked as the void region in Fig. 1(b)] is opened in the transformed space. Hence, the foundation is set for the cubical shell, comprised of six pyramidal frusta (which symmetrically surround the void region), to be designed as a cloak.

We next derive the material interpretation [13] of the space transformation given in Eq. (1) to obtain the (inhomogeneous and anisotropic) parameters of the cubical cloak. In order to calculate the material-property tensors of the cloak, we first calculate the 3×3 Jacobi matrix for the space transformation in Eq. (1) as

$$J = \begin{bmatrix} \frac{(R_2 - R_1)}{R_2} & 0 & 0 \\ \frac{-R_1 y}{x^2} & \frac{(R_2 - R_1)}{R_2} + \frac{R_1}{x} & 0 \\ \frac{-R_1 z}{x^2} & 0 & \frac{(R_2 - R_1)}{R_2} + \frac{R_1}{x} \end{bmatrix}. \quad (2)$$
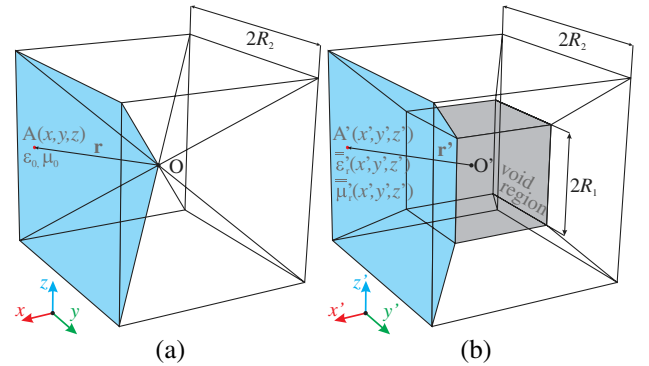

Fig. 1. (Color online) Illustration of the effects of the coordinate transformation given in Eq. (1), which leads to the construction of the cubical cloak: (a) the original space with an air-filled homogeneous isotropic cube and (b) the transformed space with a void region and an anisotropic continuously inhomogeneous cubical-shell cloak composed of six pyramidal frusta. One sixth of the cloak constructed by transformation given in Eq. (1) is highlighted in both figures.

The relative electric permittivity and magnetic permeability tensors in the transformed space, $\bar{\bar{\epsilon}}'_r$ and $\bar{\bar{\mu}}'_r$, are related to the appropriate tensors in the original space, $\bar{\bar{\epsilon}}_r$ and $\bar{\bar{\mu}}_r$, as follows [6]:

$$\bar{\bar{\epsilon}}'_r = \frac{J\bar{\bar{\epsilon}}_r J^{\mathrm{T}}}{\det(J)}, \quad \text{and} \quad \bar{\bar{\mu}}'_r = \frac{J\bar{\bar{\mu}}_r J^{\mathrm{T}}}{\det(J)}. \tag{3}$$

After simple algebra, from Eq. (3), we obtain the relative permittivity tensor components for one sixth of the cloak highlighted in Fig. 1(b):

$$\epsilon'_{r,xx} = a(R_1 - x')^2/x'^2, \qquad \epsilon'_{r,yy} = a + aR_1^2 y'^2/x'^4,$$
$$\epsilon'_{r,zz} = a + aR_1^2 z'^2/x'^4, \qquad \epsilon'_{r,xy} = \epsilon'_{r,yx} = aR_1(R_1 - x')y'/x'^3,$$
$$\epsilon'_{r,xz} = \epsilon'_{r,zx} = aR_1(R_1 - x')z'/x'^3, \quad \text{and}$$
$$\epsilon'_{r,yz} = \epsilon'_{r,zy} = aR_1^2 y'z'/x'^4, \tag{4}$$

where $a = (R_2 - R_1)/R_2$ is introduced to simplify the final expressions, and similarly for the relative permeability tensor. For constructing the remaining five parts of the cloak, an analogous procedure can be used. Alternatively, the material property tensor for one side of the cloak in Eq. (4) could be rotated around the Cartesian axes to obtain the material-property tensors for the remaining five parts of the cloak.

To validate and evaluate the properties of the constructed cubical cloak, we employ our rigorous full-wave numerical technique based on the higher-order hybrid FEM–MoM method that allows continuous variations of the material-property tensors within generally large volumetric finite elements [3,14,15]. In the numerical model, the cloaking region is modeled using building blocks in the form of a curved generalized hexahedral finite element of arbitrary geometrical orders, K_u, K_v, and $K_w (K_u, K_v, K_w \geq 1)$, shown in Fig. 2, with the position vector of a point in the element, $\mathbf{r}'(u,v,w)$, expressed in terms of Lagrange interpolation polynomials (of orders K_u, K_v, and K_w) in the parametric coordinates $-1 \leq u, v, w \leq 1$ [16]. The electric field within each element, $\mathbf{E}(u,v,w)$, is approximated by means of the curl-conforming hierarchical vector polynomial basis functions with arbitrary field approximation orders, N_u, N_v, and $N_w (N_u, N_v, N_w \geq 1)$, which are completely independent from K_u, K_v, and K_w [16], and a standard Galerkin weak-form discretization of the curl-curl electric field vector wave equation is used to obtain the system of linear equations (or a matrix equation). Utilization of high-order basis functions enables large-domain curvilinear finite element modeling (FEM hexahedra can be up to two wavelengths large in each direction). Additionally, in order to allow for the large-domain models, while also properly taking into account the continuously varying material parameters of the cloak, our FEM technique employs the same Lagrange interpolation scheme used for $\mathbf{r}'(u,v,w)$ to effectively model the continuous variations of the material-property tensors within the elements, $\bar{\bar{\epsilon}}'_r(u,v,w)$ and $\bar{\bar{\mu}}'_r(u,v,w)$, but with arbitrary material representation polynomial orders, M_u, M_v, and $M_w (M_u, M_v, M_w \geq 1)$, which are completely independent from K_u, K_v, K_w, N_u, N_v, and N_w [14]. This way, the generally adopted (and widely used by many researchers [1,6,10,11]) strategy to treat the continuously inhomogeneous media by approximating them by layers with constant permittivity and permeability (which leads to unnecessarily finer finite
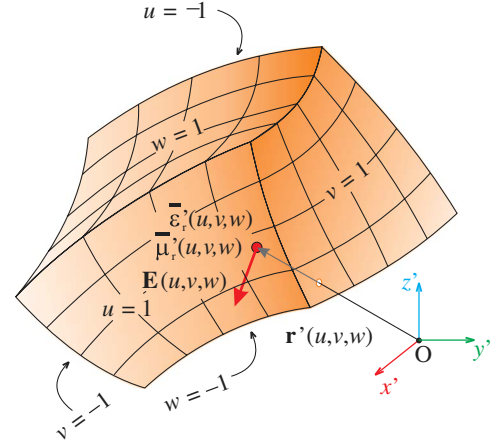

Fig. 2. (Color online) Generalized Lagrange-type parametric hexahedral finite element of geometrical orders K_u, K_v, and K_w, in the representation of the position vector $\mathbf{r}'(u,v,w)$, $-1 \leq u, v, w \leq 1$ field-approximation orders N_u, N_v, and N_w, in the approximation of the electric field vector $\mathbf{E}(u,v,w)$, and material-representation orders M_u, M_v, and M_w, to model the material parameters $\bar{\bar{\epsilon}}'_r(u,v,w)$ and $\bar{\bar{\mu}}'_r(u,v,w)$.

element meshes and a larger number of unknowns) is avoided. The strengths of the higher-order modeling can thus be fully exploited, i.e., the elements can be kept large regardless of the material-parameter variations, which ultimately results in highly efficient electromagnetic models [14]. Finally, the FEM domain truncation is achieved by coupling the FEM technique with a conformal MoM technique [17], giving rise to the hybrid higher-order, large-domain FEM–MoM technique [18].

3. NUMERICAL RESULTS AND DISCUSSION

Consider a perfect electric conductor (PEC) cubical scatterer of side length $d = 2R_1$ situated in air ($\epsilon_r = \mu_r = 1$). The scatterer is illuminated by a θ' polarized plane wave, incident from the $\theta'_{\mathrm{inc}} = 90°$ and $\phi'_{\mathrm{inc}} = 0$ direction, as shown in Fig. 3. The scatterer is coated with a cubical conformal layer (a cloak) of half-side length R_2 with material tensors $\bar{\bar{\epsilon}}'_r$ and $\bar{\bar{\mu}}'_r$ obtained from Eq. (4). The cloaking region is modeled by means of only 24 geometrically first-order ($K_u = K_v = K_w = 1$) large
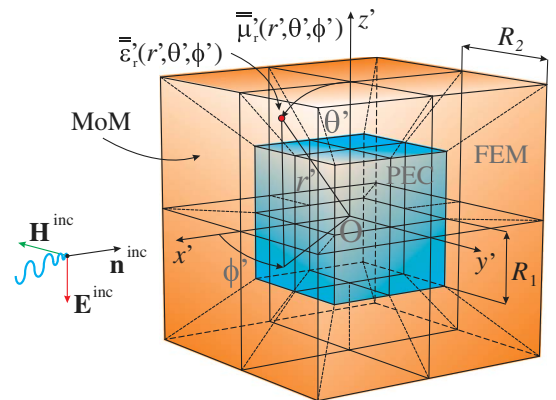

Fig. 3. (Color online) FEM–MoM model of a PEC cubical scatterer with a cubical-shell cloak: the cloak is modeled using 24 large continuously inhomogeneous anisotropic finite elements with high-order polynomial field expansions in parametric coordinates.

hexahedral finite elements (four finite elements for each pyramidal frustum), terminated by a PEC boundary condition on the inner side and by 24 large conformal geometrically first-order MoM quadrilateral patches (with equivalent surface electric and magnetic currents) on the outer side, which provide a rigorous numerical FEM domain truncation. Spatial variation of material parameters within the FEM hexahedra is approximated by the fourth-order ($M_u = M_v = M_w = 4$) Lagrange polynomials. The adopted field approximation orders are $N_u = N_v = N_w = 6$ for all FEM hexahedra, which results in only 15,564 FEM unknowns (unknown field-distribution coefficients). The adopted current approximation orders are $N_u = N_v = 5$ for all MoM patches, yielding a total of as few as 2400 MoM unknowns (unknown current-distribution coefficients). The total simulation time on a modest Windows 7 PC with Intel Core i5-760 CPU @ 2.8 GHz is around 3 min per frequency (wavelength) point. Note that the analysis of the same structure using COMSOL Multiphysics employs as many as 82,549 small finite elements and 536,968 FEM unknowns, and it failed to converge for wavelengths where $d/\lambda_0 > 0.66$ ($d = 2R_1$ and λ_0 being the cube-side length and the free space wavelength, respectively).

We assume that the cloak is thin, $R_2/R_1 = 1.1$ in Eq. (1), and show in Fig. 4 the normalized backscattering cross section, $\sigma/(R_1^2\pi)$, of the cloaked PEC cube obtained by the rigorous full-wave numerical FEM–MoM technique, against the normalized PEC cube-side length d/λ_0. The results include those for the lossless cloak as well as for lossy ones, with the loss tangent ranging from 0.0001 to 0.01, obtained with the 24-element model (shown in Fig. 3). To rigorously validate the numerical solution, the computed scattering cross section of the cube without a cloak, with the continuously inhomogeneous anisotropic FEM elements constituting the cloaking
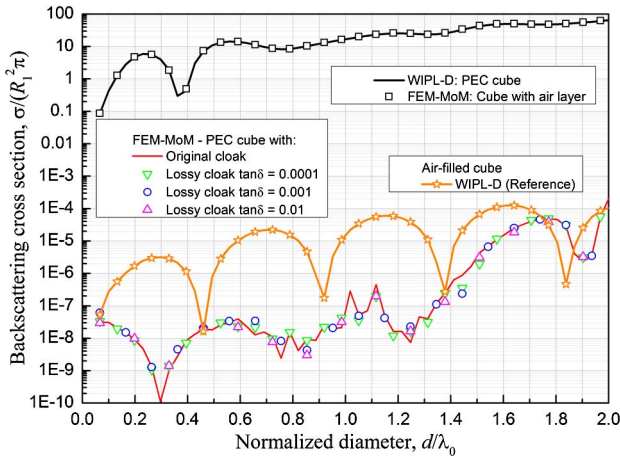

Fig. 4. (Color online) Normalized backscattering cross section of the cloaked PEC cube with $R_2/R_1 = 1.1$ in Fig. 3, including lossless (original) and lossy cloaks and an uncloaked PEC cube (the cloak shell replaced by an air layer), obtained by the higher order full-wave rigorous FEM–MoM numerical analysis versus the normalized PEC cube side length (λ_0 is the free-space wavelength). FEM–MoM results for the uncloaked PEC cubical scatterer (PEC cube with the air layer, analyzed using the same 24-element numerical model as the cloaked cube) are compared with WIPL-D results for a PEC scatterer. WIPL-D results for a homogeneous air-filled cube are also shown, as a reference for verification of the best numerical approximation of the zero backscatter from an empty cubical region of the same size as the original scatterer.
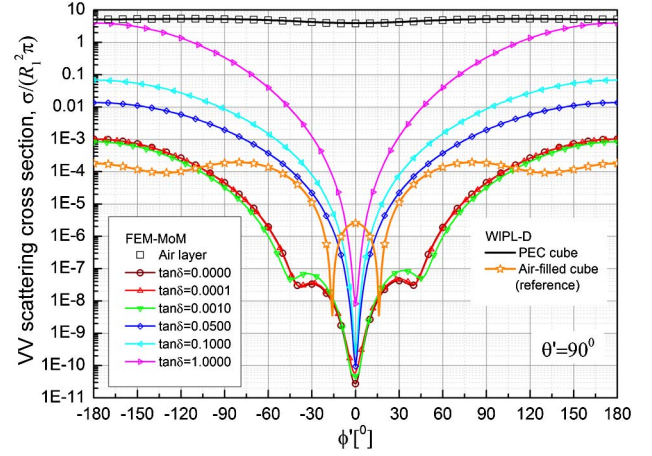

Fig. 5. (Color online) Normalized vertical–vertical (VV) scattering cross section of the cloaked (lossless and lossy, for different loss tangents) and uncloaked PEC cube in Fig. 3 ($R_2/R_1 = 1.1$, $d/\lambda_0 = 0.3$, and $d = 2R_1$), obtained by the higher-order FEM–MoM technique. The results include WIPL-D solutions for the PEC cubical scatterer and for the air-filled cube, as specified in the caption to Fig. 4.

layer being replaced by homogeneous air-filled elements having all field and current expansions and other parameters in FEM and MoM analyses the same as in the 24-element cloak model, is also shown in Fig. 4, where it is compared with the pure MoM solution obtained by the commercial software tool WIPL-D and an excellent agreement of the two sets of results is observed. In addition, a fully converged *hp*-refined WIPL-D solution for a homogeneous air-filled cube is shown as an additional reference, giving a clear insight into what the best numerical solution for the given geometry and an ideal invisibility material (scattering from free-space) would be. Based on the cloaking numerical results in Fig. 4, significant reductions (five to 10 orders of magnitude) in the scattering cross section of the cloaked PEC cube are observed in the entire analyzed range of wavelengths. While having in mind that the cloak is theoretically ideal (backscatter theoretically vanishes), we note here that the presented 24-element large-domain model yields a backscatter so low that it is on par with the best numerical approximation of the zero
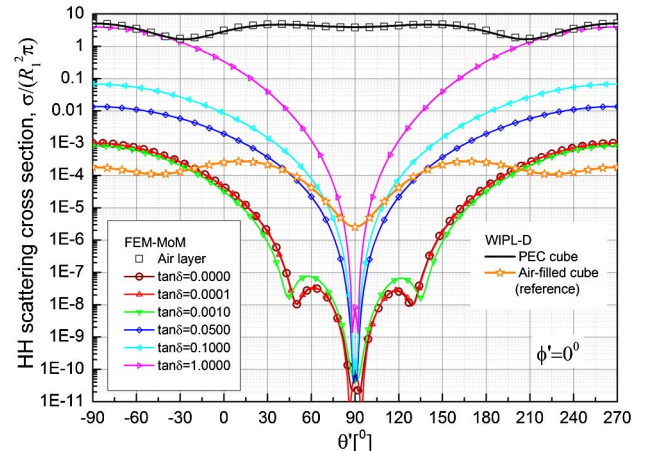

Fig. 6. (Color online) Normalized horizontal–horizontal (HH) scattering cross section of the cloaked (lossless and lossy) and uncloaked PEC cube in Fig. 3 ($R_2/R_1 = 1.1$ and $d/\lambda_0 = 0.3$), simulated by the FEM–MoM. WIPL-D results are for structures specified in the caption to Fig. 4.
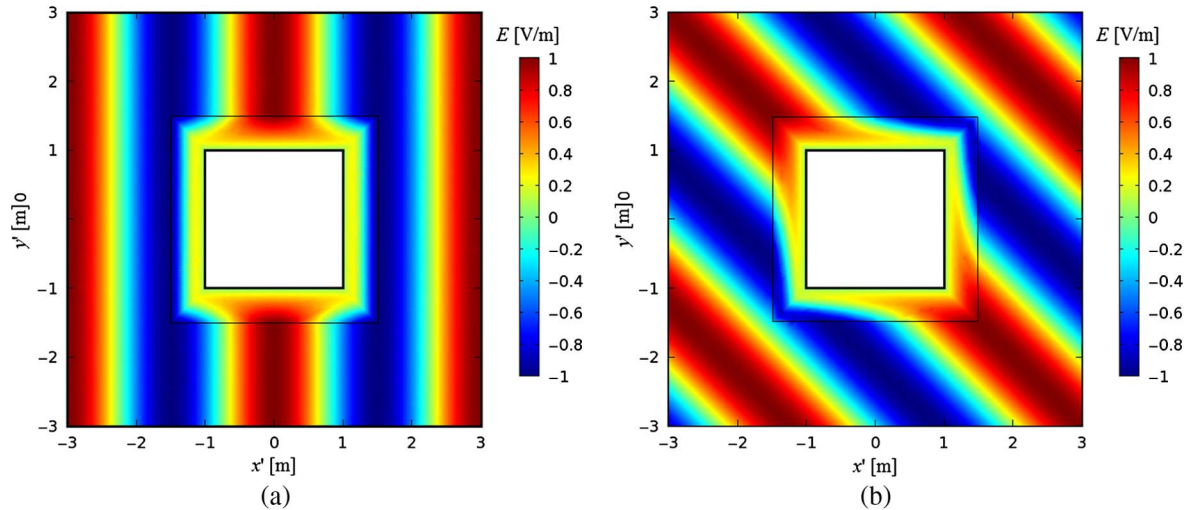
Fig. 7. (Color online) Near field (in $z' = 0$ plane) of the cloaked PEC cube in Fig. 3 ($R_2/R_1 = 1.5$ and $d/\lambda_0 = 0.66$) excited by a uniform plane wave of magnitude $E_0 = 1$ V/m, incident from the direction defined by (a) $\theta'_{inc} = 90°$, $\phi'_{inc} = 0°$ and (b) $\theta'_{inc} = 90°$, $\phi'_{inc} = 45°$.

backscatter from an empty cubical region of the same size as the original scatterer, as verified by WIPL-D and a pure surface (MoM) model. Note that the far-field numerical results for the cubical cloak are similar to or better than our results obtained for the linear spherical cloak [3], which can be attributed to the fact that, in the case of the cubical cloak, the geometrical models are exact, whereas in the spherical cloak example, the spherical geometry is approximated by the fourth-order Lagrange interpolatory functions. Finally, we can conclude that the incorporation of loss does not degrade the backscattering performance, which is consistent with the results in [1].

For the same model and incident wave shown in Fig. 3, Figs. 5 and 6 present, in two characteristic planes, the normalized scattering cross sections of the uncloaked and cloaked PEC cube with lossless and lossy cloaks, together with the reference solutions of the uncloaked PEC cube and an air-filled cubical region, all for the normalized PEC cube side length of $d/\lambda_0 = 0.3$. We observe a substantial reduction (four to 10 orders of magnitude) in σ achieved by the cloak, as well as a smooth degradation of the cloak's forward scattering performance with the increase of loss, as in [1]. The results are also consistent with those for the spherical cloak [3].

As the final example, we present the near field results for the same PEC cube with a slightly thicker cloak ($R_2/R_1 = 1.5$, so that the field in the cloak can be better observed), with the remaining modeling parameters kept the same as for the thin cloak. The near field results obtained by the higher-order FEM–MoM and COMSOL Multiphysics (shown in Fig. 7) are practically the same for the wavelength of the incident plane wave given by $d/\lambda_0 = 0.66$ (which is the shortest wavelength for which the COMSOL solution converged), and hence only one set of the results is presented. The near field solutions plotted in Fig. 7 (for the two characteristic directions of the plane wave incidence) clearly demonstrate the wave transformation in the cloaking region and validate the design goal that the cloaked structure cannot be observed from outside.

4. CONCLUSIONS

This paper has presented a novel conformal cubical, transformation-based metamaterial invisibility cloak and its rigorous

full-wave numerical validation and evaluation in both the near field and the far field based on a higher-order large domain FEM–MoM modeling approach. The numerical characterization has been carried out employing large aniso-tropic continuously inhomogeneous generalized hexahedral finite elements, with no need for a discretization of the permittivity and permeability profiles of the cloak (subdivision into very small finite elements), typical for conventional approaches to FEM analysis of transformation-based cloaks, and the analysis has required about 30 times fewer unknowns to obtain the results of a similar accuracy when compared to the COMSOL Multiphysics solution. Numerical results have shown a very substantial reduction, of five to ten orders of magnitude, in the backscattering cross section of the cloaked cube, with both lossless and lossy cloaks, in the entire analyzed range of wavelengths. They have also demonstrated the accuracy and efficiency of a simple 24-element large-domain model of the cubical cloak, yielding a backscatter so low that it is on par with the best numerical approximation of the zero backscatter from an empty cubical region of the same size as the original scatterer, as verified by WIPL-D and a pure surface (MoM) model. The fact that the far-field numerical FEM–MoM results for the cubical cloak are similar or better than the respective results for the linear spherical cloak has been attributed to an exact geometrical representation of the cubical cloak versus an approximate modeling of the spherical geometry using fourth-order Lagrange quadrilateral patches. The results have also shown the bistatic behavior of the lossless and lossy (with several characteristic loss tangents) cubical cloaks consistent with the corresponding results for the spherical and cylindrical cloaks—the incorporation of loss does not degrade the backscattering performance of the cloak, while a smooth degradation of the cloak's forward scattering performance occurs with the increase of loss in the cloak material. It is believed that the presented novel cubical cloak and its rather unconventional validation and evaluation can be of a significant interest and value in investigations of coordinate transformations needed for the conformal cloaking of cubical structures or similar objects with sharp edges and corners, as well as in development of conformal transformation-based PMLs.

ACKNOWLEDGMENTS

REFERENCES

1. S. A. Cummer, B.-I. Popa, D. Schurig, D. R. Smith, and J. Pendry, "Full-wave simulations of electromagnetic cloaking structures," Phys. Rev. E **74**, 036621 (2006).
2. J. B. Pendry, D. Schurig, and D. R. Smith, "Controlling electromagnetic fields," Science **312**, 1780–1782 (2006).
3. S. V. Savić, A. B. Manić, M. M. Ilić, and B. M. Notaroš, "Efficient higher order full-wave numerical analysis of 3-D cloaking structures," Plasmonics, online first, doi: 10.1007/s11468-012-9410-0 (posted 08 July 2012).
4. H. Chen, B.-I. Wu, B. Zhang, and J. A. Kong, "Electromagnetic wave interactions with a metamaterial cloak," Phys. Rev. Lett. **99**, 063903–063904 (2007).
5. F.-Y. Meng, Y. Liang, Q. Wu, and L.-W. Li, "Invisibility of a metamaterial cloak illuminated by spherical electromagnetic wave," Appl. Phys. A **95**, 881–888 (2009).
6. D.-H. Kwon and D. H. Werner, "Transformation electromagnetics: an overview of the theory and applications," IEEE Antennas Propag. Mag. **52**(1), 24–46 (2010).
7. J. Pendry, "Taking the wraps off cloaking," Physics **2**, 95 (2009).
8. H. Ma, S. Qu, Z. Xu, and J. Wang, "Approximation approach of designing practical cloaks with arbitrary shapes," Opt. Express **16**, 15449–15454 (2008).
9. Y. You, G. W. Kattawar, P.-W. Zhai, and P. Yang, "Invisibility cloaks for irregular particles using coordinate transformations," Opt. Express **16**, 6134–6145 (2008).
10. M. Rahm, D. Schurig, D. A. Roberts, S. A. Cummer, D. R. Smith, and J. B. Pendry, "Design of electromagnetic cloaks and concentrators using form-invariant coordinate transformations of Maxwell's equations," Photon. Nanostr. Fundam. Appl. **6**, 87–95 (2008).
11. Y. Huang, Y. Feng, and T. Jiang, "Electromagnetic cloaking by layered structure of homogeneous isotropic materials," Opt. Express **15**, 11133–11141 (2007).
12. B. Zhang, H. Chen, and B.-I. Wu, "Limitations of high-order transformation and incident angle on simplified invisibility cloaks," Opt. Express **16**, 14655–14660 (2008).
13. D. Schurig, J. B. Pendry, and D. R. Smith, "Calculation of material properties and ray tracing in transformation media," Opt. Express **14**, 9794–9804 (2006).
14. M. M. Ilić, A. Ž. Ilić, and B. M. Notaroš, "Continuously inhomogeneous higher order finite elements for 3-D electromagnetic analysis," IEEE Trans. Antennas Propag. **57**, 2798–2803 (2009).
15. A. B. Manić, S. B. Manić, M. M. Ilić, and B. M. Notaroš, "Large anisotropic inhomogeneous higher order hierarchical generalized hexahedral finite elements for 3-D electromagnetic modeling of scattering and waveguide structures," Microw. Opt. Technol. Lett. **54**, 1644–1649 (2012).
16. M. M. Ilić and B. M. Notaroš, "Higher order hierarchical curved hexahedral vector finite elements for electromagnetic modeling," IEEE Trans. Microw. Theor. Tech. **51**, 1026–1033 (2003).
17. M. Djordjević and B. M. Notaroš, "Double higher order method of moments for surface integral equation modeling of metallic and dielectric antennas and scatterers," IEEE Trans. Antennas Propag. **52**, 2118–2129 (2004).
18. M. M. Ilić, M. Djordjević, A. Ž. Ilić, and B. M. Notaroš, "Higher order hybrid FEM–MoM technique for analysis of antennas and scatterers," IEEE Trans. Antennas Propag. **57**, 1452–1460 (2009).